A Measurement-Based Design Equation for the Attenuation of MMIC-Compatible Coplanar Waveguides

George E. Ponchak, Mehran Matloubian, and Linda P. B. Katehi

***Abstract*—Measured attenuation of coplanar waveguide (CPW) transmission lines with narrow strip and slot widths fabricated on GaAs, high-resistivity Si, and InP is used to derive a new closed-form equation to calculate line losses. This new equation is shown to be more accurate than previous expressions, yet simple enough to be programmed into a hand-held calculator since it is based on a simple relationship between attenuation and the product of the strip and slot widths. The derived equation is applicable to CPW's with aspect ratio and metal thicknesses commonly used in monolithic microwave integrated circuits.**

***Index Terms*—Attenuation, coplanar waveguide, microwave transmission lines.**

I. Introduction

Coplanar waveguides (CPW's) are used extensively in millimeter-wave and monolithic microwave integrated circuits (MMIC's) because they are uniplanar, which allows easy connection of shunt and series circuit elements without via holes. This eliminates the requirement for backside wafer processing and significantly lowers the fabrication cost. Another way to keep cost low is to meet design specifications on the first pass, which requires accurate design equations. Commercial software tools based on finite-element, method-of-moments, or finite-difference time-domain techniques are required to design CPW circuits. While these techniques are capable of determining the characteristic impedance and propagation constant accurately, they fail to provide realistic estimates of the line loss. In the literature, closed-form equations for the determination of CPW attenuation have been derived using Wheeler's incremental inductance rule [1], numerical fitting of modified spectral-domain-analysis results [2], integration of the current density over the conducting strips [3]–[7], and a quasi-TEM circuit analysis [8], but they all suffer from limitations in accuracy and/or complexity. Typically, these equations require the calculation of elliptic integrals of modulus $k = S/(S + 2W)$ where S and W are the strip and slot widths, respectively, as shown in Fig. 1, as well as S and W individually, resulting in complicated expressions. More importantly, there has not been a comparison made between each of the closed-form equations and a single set of measured data to provide an estimation of their accuracy.

In this paper, we report a new closed-form equation for the attenuation of CPW lines compatible with MMIC design. The equation is derived by curve fitting measured data and is based on a newly found relationship between attenuation and the product of the center strip and slot widths. The new equation is valid over the measured frequency range of 1–40 GHz and for metal thickness between 0.5 and 3.0 μm. It does not involve elliptic integrals, is simple to use, and is easily invertible to determine the optimum CPW geometry that results in low loss and small size. To provide an indication of the accuracy of this new equation and the equations in the literature, the average root-mean-square error between measured data and the predicted attenuation for CPW lines with $10 \leq S \leq 80$ μm and $t = 1.5$ μm over the frequency range of 1–40 GHz is presented.

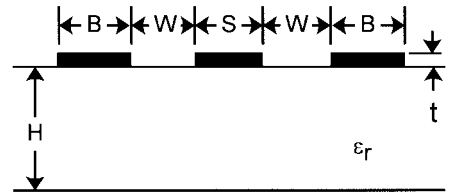

Fig. 1. Schematic of CPW.

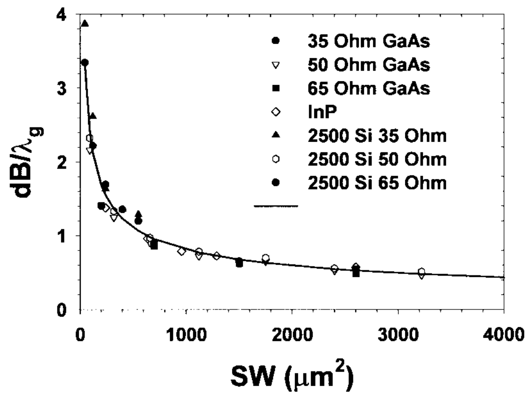

Fig. 2. Measured attenuation per wavelength at 23 GHz as a function of SW for CPW lines fabricated on GaAs, InP, and high-resistivity Si with a metal thickness of 1.58 μm.

II. Measurement Technique

CPW transmission lines are fabricated on: double-side polished Si wafers with $\rho \geqslant 2500\ \Omega \cdot$ cm, $H = 360$ μm, and $\varepsilon_r = 11.9$, GaAs wafers with $H = 500$ μm and $\varepsilon_r = 12.85$, and InP wafers with $H = 600$ μm and $\varepsilon_r = 12.4$. Front-side metal consists of 0.02 μm of Ti and electron-beam evaporated Au with a thickness t of 0.49, 1.5, and 2.22 μm. No backside ground plane is used. Transmission lines with aspect ratio $k = S/(S + 2W)$ between 0.2–0.7, characteristic impedances between 35–65 Ω, and center strip widths between 10–80 μm are characterized. The ground-plane width B is equal to $4S$ for each line to assure that the results are independent of the ground-plane width without exciting spurious resonances [9]. Lastly, since $H \geqslant 3(S + 2W)$ for all of the lines, the results are independent of the substrate thickness.

Measurements are performed on an HP 8510C Vector Network Analyzer with a probe station and GGB Industries probes. A quartz spacer is placed between the wafer and the wafer chuck to isolate the circuits from the backside ground plane and prevent the excitation of parasitic parallel-plate waveguide modes. To determine the CPW attenuation α and effective permittivity $\varepsilon_{\mathrm{eff}}$, a thru-reflect-line (TRL) calibration routine [10] is used with four delay lines, the longest line being 1.0 cm, to cover the entire frequency range of 1–40 GHz and to minimize measurement errors. Further reduction of random errors

Manuscript received December 30, 1997; revised October 5, 1998. This work was supported by the Defense Advanced Research Projects Agency (DARPA) and by Hughes Research Laboratory.

G. E. Ponchak is with the Electron Device Technology Branch, NASA Lewis Research Center, Cleveland, OH 44135 USA.

M. Matloubian is with Hughes Research Laboratory, Malibu, CA 90265 USA.

L. P. B. Katehi is with the Department of Electrical Engineering and Computer Science, The University of Michigan at Ann Arbor, Ann Arbor, MI 48109-2122 USA.

Publisher Item Identifier S 0018-9480(99)01143-6.

TABLE I
AVERAGE ROOT-MEAN-SQUARE ERROR BETWEEN MEASURED AND CALCULATED ATTENUATION ACROSS THE FREQUENCY BAND OF 1–40 GHz FOR CPW LINES FABRICATED ON GaAs WITH METAL THICKNESS OF 1.58 μm $\sigma = 4.1 \cdot 10^7$ S/m USED TO CALCULATE ATTENUATION

S(μm)	W(μm)	Gupta [1]	Liao [2]	Collin [3]	Holloway [7]	Heinrich [8]	This work, Eqns.1-3
10	4.5	0.566	0.220	0.177	0.248	0.154	0.018
20	6	0.497	0.236	0.124	0.177	0.088	0.018
30	8	0.423	0.258	0.111	0.150	0.076	0.034
40	10	0.416	0.253	0.080	0.111	0.046	0.028
50	11	0.420	0.259	0.074	0.093	0.042	0.031
10	9	0.427	0.120	0.085	0.143	0.087	0.022
20	16	0.362	0.141	0.083	0.062	0.040	0.037
30	22	0.372	0.135	0.111	0.035	0.070	0.055
40	28	0.392	0.124	0.141	0.057	0.106	0.069
50	35	0.301	0.177	0.119	0.050	0.082	0.031
60	40	0.415	0.128	0.184	0.105	0.165	0.070
70	46	0.446	0.131	0.215	0.143	0.209	0.082
80	51	0.446	0.140	0.224	0.153	0.222	0.069
10	20	0.304	0.083	0.088	0.076	0.054	0.043
20	35	0.306	0.084	0.123	0.044	0.068	0.045
30	50	0.332	0.094	0.163	0.081	0.123	0.058
40	65	0.387	0.117	0.216	0.142	0.200	0.082
average	error	0.401	0.159	0.136	0.110	0.108	0.047

is accomplished by repeating the characterization of each set of test circuits three times and averaging α and ε_{eff}.

III. RESULTS

Although previous closed-form equations relate the attenuation to the parameter k, it is shown in Fig. 2 that the measured attenuation per guided wavelength is inversely proportional to the product of the center conductor and slot widths $\alpha \propto 1/(SW)$. In fact, the attenuation per unit length has the same relationship, but plotting attenuation in dB/λ_g permits the data from each of the three substrate types to be combined onto a single plot. To derive a closed-form equation for the attenuation of a CPW, $\alpha = af^b$ [11] is assumed, which is found to give good agreement for frequencies above 2–4 GHz. From the measured data, the new closed-form equation is found to be

$$\alpha = af^b \text{ (dB/cm)} \tag{1}$$

$$a = \sqrt{\frac{\varepsilon_r + 1}{2}}\left[\frac{45.152}{(SW)^{0.410}e^{2.127\sqrt{t}}}\right] \tag{2}$$

$$b = 0.183(t + 0.464) - 0.095k_t^{2.484}(t - 2.595) \tag{3}$$

where S, W, and t are in micrometer, f is in gigahertz, and k_t [12] is

$$k_t = \frac{S + \Delta t}{S + 2W - \Delta t}$$

$$\Delta t = \frac{1.25t}{\pi}\left[1 + \ln\frac{4\pi S}{t}\right].$$

Equations (1)–(3) are valid for $0.5 < t < 3.0$ μm, $0.2 < k < 0.7, 10 < S < 80$ μm, and $1 < f < 40$ GHz, which covers the range of parameters commonly used for MMIC design. Since these equations are derived from measured attenuation, they account for conductor, dielectric, and radiation loss, but the measurements show that conductor loss dominates for the GaAs and InP substrates. For the Si wafers, the fitting parameters "a" and "b" are dependent on the resistivity of the Si substrates. Thus, the utility of these equations for Si is limited to the case of $\rho > 2500$ $\Omega \cdot$ cm where the resistivity dependence is very small.

The accuracy of (1)–(3) is first verified by comparing the measured attenuation for GaAs of this paper, the measured attenuation for CPW lines on InP with $t = 0.5$ μm of [11], and the predicted attenuation from (2). This is shown in Fig. 3, where it is seen that the measured data is accurately described by (2). The InP data were not corrected for the slightly lower permittivity. Measured attenuation in [11] for CPW lines on InP with $t = 0.25$ μm did not follow the relationship shown in Fig. 2 and, thus, is not used here.

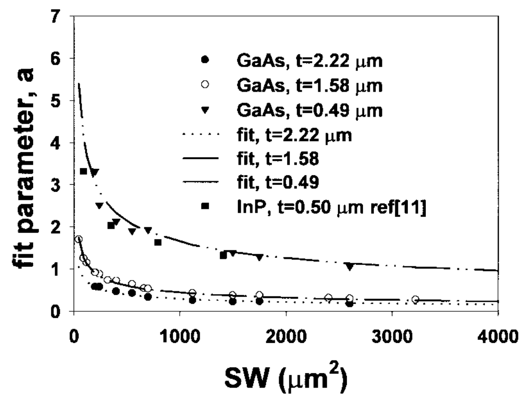

Fig. 3. Fitting parameter "a" from $\alpha = af^b$ for CPW lines as a function of SW and t.

Further verification of the accuracy of the newly derived closed-form equations is found by calculating the normalized difference between the measured and calculated attenuation $|\alpha_{\text{meas}} - \alpha_{\text{calc}}|/\alpha_{\text{meas}}$ at 201 points across the frequency range of 1–40 GHz for each of the 17 combinations of S and W measured (see Table I for the geometries measured). The same analysis is performed on the other equations and shows that the equation based on Wheeler's incremental inductance rule [1] overestimates the attenuation by as much as 60% at the upper end of the frequency range, while the attenuation predicted by Liao and Collin underestimate the attenuation at low frequencies. These errors can be attributed to the assumption of $t \gg \delta$ and large S that was made in each case to justify the $\sqrt{f}$ dependance. Although Liao's frequency dependance varies with the CPW geometry, it is approximately $\sqrt{f}$ for the lines measured in this paper. For the CPW lines measured here, b ranged from 0.38 for 65-Ω lines with wide center strips to 0.45 for 35-Ω lines with narrow strips. Thus, the thick-metal-line assumption introduces an error between 55% and 20%, which agrees with the measurements. The equations from Holloway and Heinrich do not make the thick-metal assumption and the normalized error for them is nearly independent of frequency.

The average root-mean-square error from 1 to 40 GHz for 17 different CPW lines on GaAs with a metal thickness of 1.58 μm is shown in Table I. It is seen that of the previous equations in the literature, those in [7] and [8] are the most accurate with an average error of approximately 11%, whereas an average error of 40% and a maximum error of 56% is obtained using Wheeler's incremental inductance rule. The average error for (1)–(3), shown in Table I, is only 4.7%, and if all three metal thickness are included, the average error is 6%. This is better than any of the previously reported equations, and most of this error is at low frequency where af^b does not accurately fit the data, as discussed earlier; the maximum error is 35% at 1 GHz for the thickest metal lines.

IV. Conclusions

This paper has presented a new closed-form equation for the prediction of CPW attenuation that is valid for a wide range of center strip conductor widths, slot widths, and metal thickness. It has been shown that this simple equation is as accurate as more complicated closed-form equations with an average error from 1 to 40 GHz of approximately 6%. Furthermore, the equation is invertible if one assumes f^b varies slowly with S and W to permit a determination of SW required to achieve a desired attenuation. A comparison between five previous closed-form equations for CPW attenuation to measured data has been made.

References

[1] K. C. Gupta, R. Garg, and I. J. Bahl, *Microstrip Lines and Slotlines*. Norwood, MA: Artech House, 1979, pp. 275–287.

[2] C.-L. Liao, Y.-M. Tu, J.-Y. Ke, and C. H. Chen, "Transient propagation in lossy coplanar waveguides," *IEEE Trans. Microwave Theory Tech.*, vol. 44, pp. 2605–2611, Dec. 1996.

[3] R. E. Collin, *Foundations for Microwave Engineering*. New York: McGraw-Hill, 1992, pp. 905–910.

[4] G. Ghione, "A CAD-oriented analytical model for the losses of general asymmetric coplanar lines in hybrid and monolithic MIC's," *IEEE Trans. Microwave Theory Tech.*, vol. 41, pp. 1499–1510, Sept. 1993.

[5] R. Goyal, Ed., *Monolithic Microwave Integrated Circuits: Technology & Design*. Norwood, MA: Artech House, 1989, p. 375.

[6] G. H. Owyang and T. T. Wu, "The approximate parameters of slot lines and their complement," *IRE Trans. Antennas Propagat.*, vol. AP-6, pp. 49–55, Jan. 1958.

[7] C. L. Holloway and E. F. Kuester, "A quasi-closed form expression for the conductor loss of CPW lines, with an investigation of edge shape effects," *IEEE Trans. Microwave Theory Tech.*, vol. 43, pp. 2695–2701, Dec. 1995.

[8] W. Heinrich, "Quasi-TEM description of MMIC coplanar lines including conductor-loss effects," *IEEE Trans. Microwave Theory Tech.*, vol. 41, pp. 45–52, Jan. 1993.

[9] G. E. Ponchak, E. M. Tentzeris, and L. P. B. Katehi, "Characterization of finite ground coplanar waveguide with narrow ground planes," *Int. J. Microcircuits and Elect. Pack.*, vol. 20, no. 2, pp. 167–173, 1997.

[10] R. B. Marks, "A multiline method of network analyzer calibration," *IEEE Trans. Microwave Theory Tech.*, vol. 39, pp. 1205–1215, July 1991.

[11] W. H. Haydl, J. Braunstein, T. Kitazawa, M. Schlechtweg, P. Tasker, and L. F. Eastman, "Attenuation of millimeter-wave coplanar lines on gallium arsenide and indium phosphide over the range 1–60 GHz," in *IEEE Int. Microwave Symp. Dig.*, June 1992, pp. 349–352.

[12] K. C. Gupta, R. Garg, and R. Chadha, *Computer-Aided Design of Microwave Circuits*. Norwood, MA: Artech House, 1981.

A New Phase-Shifterless Scanning Technique for a Two-Element Active Antenna Array

Young-Huang Chou and Shyh-Jong Chung

***Abstract*—In this paper, a new phase-shifterless beam-scanning technique is proposed and demonstrated for a two-element active antenna array. An internal control line with an embedded amplifier is introduced in the array to provide another injection signal other than the mutual-coupling injection signal between antennas. By mixing the effects of the signals from the control line and mutual coupling, the phase difference between antennas is adjusted by gradually changing the amplifier bias on the control line. A dynamic analysis is presented to explain the scanning mechanism. The measured results showed that, when the control-line amplifier was biased from the off state to fully on state, the radiation pattern of the array was varied smoothly from the out-of-phase mode (with 180° radiation phase difference) to the in-phase mode (with 0° phase difference). During the scanning process, the antenna oscillators were stably locked, with the deviation of the locked frequency lower than 0.35%.**

***Index Terms*—Active antenna array, phase-shifterless scattering.**

I. Introduction

In the applications of microwave and millimeter-wave systems, the spatial or quasi-optical power-combining techniques are used increasingly for high-power generation and low-loss transmission with the limitation of available power of solid-state devices [1], [2]. Active integrated antennas, which combine passive antennas with active circuits, are implemented in an array to fulfill these requirements. Each active antenna acts not only as a radiator, but also an oscillator. By means of the injection-locking signals, these oscillators can be synchronized to a common frequency and the powers radiated from the antennas can be effectively combined in free space. Two types of injection-locking distribution have been used in the literature. In the first type, the injection signals come from the mutual couplings between array elements, either through free space (weak coupling) [3], [4] or through an embedded coupling network (strong coupling) [5]. Depending on the inter-element distance, the phase delay between adjacent antennas can be locked to an in-phase mode (with 0° phase delay) or an out-of-phase mode (with 180° phase delay) [3], [5]. In the second type, the injection signals originate from an external oscillator and are distributed to all the oscillators in the array [6]. The phase delay is determined by the path-length differences of the injection signals to the oscillators, so that the array radiation field can be focused to a predesigned direction.

In addition, the beam-scanning ability for these active antenna arrays has recently become attractive. By taking the advantages of the injection-locking nonlinear effect to alter the phase delay progressively, the array radiation beams can be scanned without using expensive phase shifters [4], [5], [7]–[9]. Stephan first demonstrated the beam-scanning phenomenon by adjusting the phases of the external signals injected to the peripheral active antennas of the array [7]. Since the total phase delay from the first to last antennas was bounded by the phase difference between the two external injection signals, the beam-scanning range was thus limited and inversely

Manuscript received February 23, 1998; revised October 17, 1998. This work was supported by the National Science Council of the Republic of China under Grant NSC 87-2215-E-009-064.

The authors are with the Department of Communication Engineering, National Chiao Tung University, Hsinchu, Taiwan 300, R.O.C.

Publisher Item Identifier S 0018-9480(99)01142-4.